PROCEEDINGS OF THE ROYAL SOCIETY A

rspa.royalsocietypublishing.org

Research

Article submitted to journal

Subject Areas:
xxxxx, xxxxx, xxxx

Keywords:
xxxx, xxxx, xxxx

Author for correspondence:
A. Champneys
e-mail: a.r.champneys@bristol.ac.uk

Royal Society Publishing
Informing the science of the future

The Two-Ball Bounce Problem

Y. Berdeni, A. Champneys and R. Szalai

Department of Engineering Mathematics, University of Bristol, Queen's Building, University Walk, Bristol BS8 1TR, UK

A popular classroom demonstration is revisited in which a light ball and a much larger heavier ball are vertically aligned and dropped together onto a hard surface. Careful experimental data obtained using a high-speed camera is compared to a lumped-mass Newtonian restitution model. Good macroscopic agreement is found, provided there is sufficient separation between the two balls as they are dropped. An alternative continuum model based on elastic membrane theory is developed to explain the limit in which the balls are initially touching. The model assumes an elastic wave to be set up in the lower ball upon its impact with the floor which subsequently launches the upper ball, like a particle on a trampoline, before the lower ball leaves the ground. A favourable comparison with experimental data is found for the case of negligible initial separation between the balls.

1. Introduction

Impact mechanics — characterised by contacts between (nearly) rigid bodies that have brief duration, high force levels, rapid dissipation of energy, and large accelerations and decelerations — is of great concern in many practical engineering problems; see e.g. [1–5] and references therein. This paper considers in detail a canonical impact problem, namely the impact of two balls placed vertically above one another and dropped onto a hard floor. This problem has been studied for more than 40 years; in particular the case of a small mass ratio μ between the two balls where the upper one can end up with a counter-intuitively high rebound velocity, see e.g. [6–8].

Using Newtonian impact theory, there is a simple explanation of this phenomenon [9–11], which we reproduce in §2 below. That theory predicts the post-impact velocity of the upper ball to approach $(e_{12} + e_2 + e_{12}e_2)$ times its pre-impact velocity in the limit $\mu \to 0$, where e_{12} and e_2 are coefficients of restitution between the two balls and between the lower ball and the floor respectively. However the theory assumes a certain well-defined order of instantaneous collisions. That is, one

assumes there to be a small initial separation Δx between the two balls, so that the lower one first impacts with and leaves the floor before it impacts with the upper ball. In practice though, no impact is ever instantaneous and such an assumption is not valid if the two balls are initially touching. In what follows, we shall refer to this Newtonian impact model as the independent collision model (ICM).

(a) Experimental methodology.

To test the ICM predictions, we have conducted detailed, quantitative laboratory experiments using a variety of different spherical (and, for the upper 'ball', non-spherical) bodies with data recorded using high speed photography; see Fig. 1. To ensure that both bodies were vertically aligned correctly, a drop tower was used to secure the bodies in position before their release. A different design was made for the tubular lower portion of the tower, for each kind of lower ball used, in each case slightly wider than that ball's diameter. The upper body was placed in the upper portion of the drop tower, ensuring that the two centres of mass were vertically aligned. Each body was held in place by a pin that formed the armature of an electromechanical solenoid, attached to a pre-compressed spring. Current passing through the solenoid would further compress the spring, causing the pin to lose contact with the body, thus allowing it to fall freely under gravity. In this way the timing of each ball's release could be carefully controlled. The drop tower was held rigidly above a smooth rigid concrete floor. In order to vary the velocity of impacts, the height of the drop tower above the floor was adjusted in the range from 0.2 m to 1 m. The separation distance between the two balls could also be finely varied through adjustment of the vertical position of the upper pin.

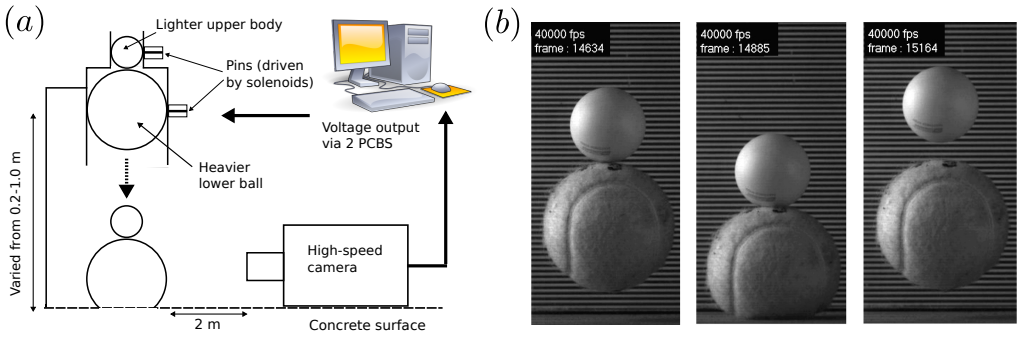

Figure 1. (a) A schematic of the experimental set-up. (b) Stills from high-speed camera for an instance of the 'two-ball bounce problem', in this case a tennis ball and a table tennis ball impact.

To obtain quantitative data, a high-speed camera was positioned two metres away in order to capture the motion of the bodies in the vicinity of the floor. Data was recorded at a rate of $20,000$ frames per second. Frame-by-frame and pixel-by-pixel analysis of the image data enabled accurate estimation of the velocity of each ball immediately prior to contact being initiated and immediately after it was broken. The apparent outline of the deformation of the lower ball was also recorded during the entire impact process.

In order to use the ICM predictively, the two coefficients of restitution e_2 and e_{12}, were measured independently. As will be seen in §2, we have found that the ICM model prediction for the rebound velocities is remarkably accurate, provided the initial separation between the two balls Δx is large enough. In the case where the two balls are touching or almost touching though, we find that the ICM model over-predicts the rebound velocity of the upper ball.

(b) Previous studies

An early prior attempt to extend the ICM model to describe what happens in the the two-ball bounce problem is the work of Harter [8]. He tried to explain the experimental results for the case where the lower ball is a superball and the upper body is a pen inserted into another superball. He found acceptable agreement by modelling each body as a nonlinear neo-Hookeian spring, with the nonlinear coefficients fit to experimental data.

More than twenty years later Patrício [11] attempted a rational derivation of a nonlinear-spring model, assuming a Hertzian contact (see [12]) between two spherical objects and between the lower sphere and the ground. This leads to two nonlinear ordinary differential equations (ODEs) that depend on the mass ratio μ and a rigidity ratio ν. The rebound velocities predicted for different mass ratios were found to be broadly similar to those from the ICM model, except in the limit that either μ or ν tends to zero. In particular, as $\mu \to 0$ the ICM predicts that the upper ball rebound velocity will be maximal, whereas the Patríco's theory predicts it be minimal, with both balls behaving as if they were a single body. We have not observed such behaviour in our experiments.

Cross [10] considered a linearised version of a stiff-spring model to explain experimental data for the two-ball bounce between a basketball and a tennis ball. He found that numerical solutions of the spring model were consistent with results obtained from a nonlinear Hertzian model with the same mass and rigidity ratios. However, using measured values of masses and rigidity led to rebound velocities that were very different from those observed. Modifying the spring model to account for energy losses and fitting a separation distance between the balls gave a better fit with data for the case of impacts between superballs. Müller and Pöschel [9] undertook a similar modelling study in which they added a linear spring and dashpot to each collision in the ICM. They found though that in the limit $\Delta x \to 0$, such a model predicts multiple collisions to occur between the two balls, before they finally separate. We have found no example of such multiple collisions occurring in our experimental results where we always have a lighter upper ball. However, in our data we relied upon measurements of position and never directly measured the contact force. There is evidence from measuring the force waveforms between the two balls that multiple collisions occur in cases (not considered in this scope of this paper) where the upper ball is heavier (see [10]).

In fact, Cross [10] found that simply using the ICM and fitting a single restitution parameter e for both collisions led to a much better fit with experimental results for the basketball and tennis ball collision than the conservative mass-spring model. However, our results in §4 suggest that the two impacts would not be independent for this experiment. In reality, the basketball would still be in contact with the floor when the tennis ball hit it and so the assumptions of the ICM would be violated.

As a clue to why these discrepancies between theory and experiment may arise, it is interesting to note that even a problem as simple as the impact of a single sports ball on a hard surface is highly non-trivial; see for example [13–16]. For such a problem, Stronge *et al* [17] recently developed a viscoplastic model for the dissipation of energy between colliding bodies and compared it favourably with experimental data for various different sports balls.

The problem of two and three-body impact has been extended to multi-body chain collision. For example Hinch *et al* [18] studied two different laws for the contact force in a Newton's cradle, in which a single ball impacts with a chain of balls. Using either a simple linear compression law or a nonlinear Hertzian contact law they were able to define a continuum partial differential equation (PDE) model for the case of an infinite chain. More recently Boechler *et al* modelled a one-dimensional diatomic granular crystal composed of compressed elastic beads as a chain of nonlinear oscillators [19]. There, solitary waves of force are found, over many particle diameters, that can be described by KdV-like models.

The fundamental tenet of this paper then is that lumped mass models for the process of the two-ball bounce problem are not likely to contain sufficient complexity to describe the processes that occur for if the two balls remain in contact when the lower ball hits the floor. It would seem

that we need to consider at least the lower ball as a continuum elastic body. The key is to describe the response of the upper portion of the lower ball to the elastic waves that are triggered by the impact of the bottom of the ball with the floor. Such an analysis is greatly simplified in the case that the upper ball is of significantly lower mass, and is also the limit in which high rebound velocities are observed experimentally.

(c) Outline

The purpose of the present study is to derive a consistent continuum model for the two-ball bounce problem in the limit of small mass ratio. We shall also compare such a model's predictions with experimental results obtained using the method outlined above.

The rest of this paper is outlined as follows. In §2 we briefly derive the independent collision model (ICM) and present some preliminary experimental data to show the extent of the validity of its predictions. §3 then develops a continuum elastic model (CEM) taking care to derive consistent initial and terminal conditions to enable calculation of the lift-off velocity of the upper ball. §4 contains further experimental data in cases where the lower ball is either a tennis ball or a basketball and the upper ball is a number of different much lighter objects. Parameters of the CEM are carefully fit and a favourable comparison found for the lift-off velocity in the case that the balls are initial touching, or almost touching. Finally, §6 draws conclusions and seeks to put the results in context.

2. The Independent Collision Model

Consider two spherical rigid bodies with masses m_1 and m_2, and radii r_1 and r_2, respectively. Shortly we shall be interested in the case that $m_1 \ll m_2$, and $r_1 \ll r_2$. The balls are released from an initial resting position in vertical alignment with initial heights x_1 and x_2 above a rigid surface, with $\Delta x := x_1 - x_2 - r_1 - r_2 \geq 0$, see Fig. 2. During free-fall we presume the only force acting on either ball is gravity, $g = 9.81\text{ms}^{-2}$. We also assume that all impacts occur instantaneously and obey Newton's law of restitution with coefficients e_{12} between the two balls and e_2 between the lower ball and the ground.

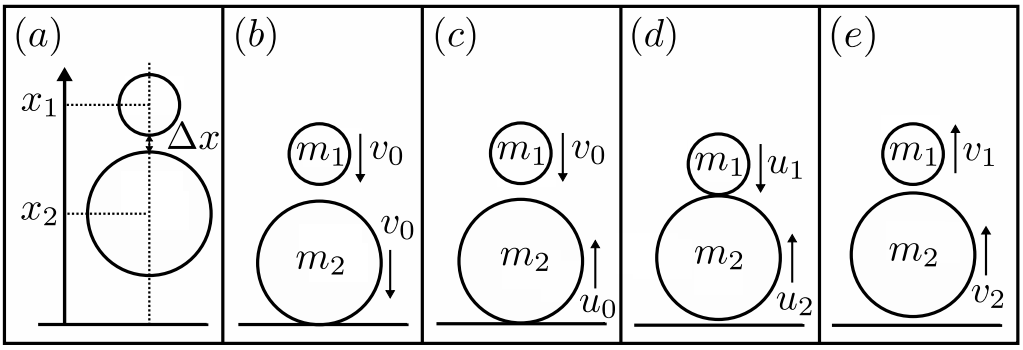

Figure 2. The Independent Collision Model. Two independent collisions are assumed; the lower ball independently impacts with the ground and then collides with the upper body.

Under these assumptions, the lower sphere impacts with the ground at time $t_0 = \sqrt{2(x_2 - r_2)/g}$ with velocity $v_0 = -\sqrt{2g(x_2 - r_2)}$ and rebounds with velocity

$$u_0 := -e_2 v_0 = e_2 \sqrt{2g(x_2 - r_2)}. \tag{2.1}$$

The velocity $u_0 > 0$ is positive and the velocity of the upper sphere is v_0 which is negative, and they are separated by a distance Δx, so they must subsequently impact. This second impact takes

place at time

$$t_1 = t_0 - \frac{\Delta x}{(1+e_2)v_0} := t_0 + \Delta t. \tag{2.2}$$

So the velocity prior to impact for the upper ball is $u_1 = -gt_1$ and for the lower ball is $u_2 = u_0 - g\Delta t$.

From the law of conservation of momentum we have

$$m_1u_1 + m_2u_2 = m_1v_1 + m_2v_2, \tag{2.3}$$

where v_1 and v_2 represent the post-impact velocities of bodies 1 and 2 respectively. Now, by definition, the coefficient of restitution between the two bodies

$$e_{12} := \frac{v_2 - v_1}{u_1 - u_2}. \tag{2.4}$$

Now we can solve (2.3) and (2.4) simultaneously for the two unknowns v_1 and v_2 to obtain the post-impact velocities

$$v_1 = \frac{\mu u_1 + u_2 + e_{12}(u_2 - u_1)}{\mu + 1} \quad \text{and} \quad v_2 = \frac{\mu u_1 + u_2 + \mu e_{12}(u_1 - u_2)}{\mu + 1}, \tag{2.5}$$

where we have defined the mass ratio as $\mu := m_1/m_2$.

In the limit of small separation $\Delta x \to 0$ we have

$$v_1 \to \frac{\mu - e_2 - e_{12}(1+e_2)}{\mu + 1}\, v_0 \qquad \text{and} \quad v_2 \to \frac{\mu - e_2 + \mu e_{12}(1+e_2)}{\mu + 1}\, v_0. \tag{2.6}$$

Then, in the limit of a small mass ratio $\mu \to 0$ we have

$$v_1 \to -((1+e_2)e_{12} + e_2)v_0, \qquad \text{and} \quad v_2 \to -e_2v_0. \tag{2.7}$$

Hence, for a pure elastic collision ($e_2 = e_{12} = 1$) we have that $v_1 \approx -3v_0$ and $v_2 \approx -v_0$ so that the upper ball lifts off with three times its original velocity. A simple balance of kinetic and gravitational energy then recovers the classical result [9,10] that the upper ball bounces to nine times the height from which it was dropped, whereas the lower, much heavier, ball is unaffected and returns to its original height.

More generally, the formulae (2.5) can also be used to predict the velocities of v_1 and v_2 of both balls for a general mass ratios μ, coefficients of restitution e_2 and e_{12}. and separation distance Δx. All of these quantities can be measured independently, Then by direct measurement of the initial velocity v_0 of the balls, the predicted rebound velocities can be compared to the measured data. The quantity Δt (2.2) gives an expression for the time between the lower ball hitting the ground and the upper ball lifting off as a function of the initial separation Δx. As the ICM assumes instantaneous collisions the predicted impact duration of the entire two-ball impact sequence is simply Δt, which can be compared to the experimental observations.

Fig. 3 shows experimental data obtained for the case of a basketball and a tennis-ball, for which we measured $\mu = 0.1007$, $e_2 = 0.80$ and $e_{12} = 0.89$. We collected data for separation distances between 0 and 70 mm and initial heights from 0.2 to 1 m. Fig. 3 depicts the ratio of post impact velocity to the immediate pre-impact velocity of both balls, $|v_i/v_0|$, as a function of Δx for $x_2 = 1$ m. Little discernible dependence on the magnitude of v_0 was found. Also plotted in the figure is the ICM prediction. Note from the vertical red line that for $\Delta x < 120$ mm we found that the lift-off of the upper ball occurred before the lower ball had left contact with the floor (which happens after about 0.03s).

Note how accurate the prediction of the ICM model is for $\Delta x > 10$ mm, despite the fact that the assumptions of the theory, namely that the impact of lower ball with floor and between the two balls are well separated temporally, are incorrect for this range of Δx. However, there is a different cluster of points for $\Delta x < 10$ mm in which there is significantly lower v_1 and higher v_2 than predicted by the ICM.

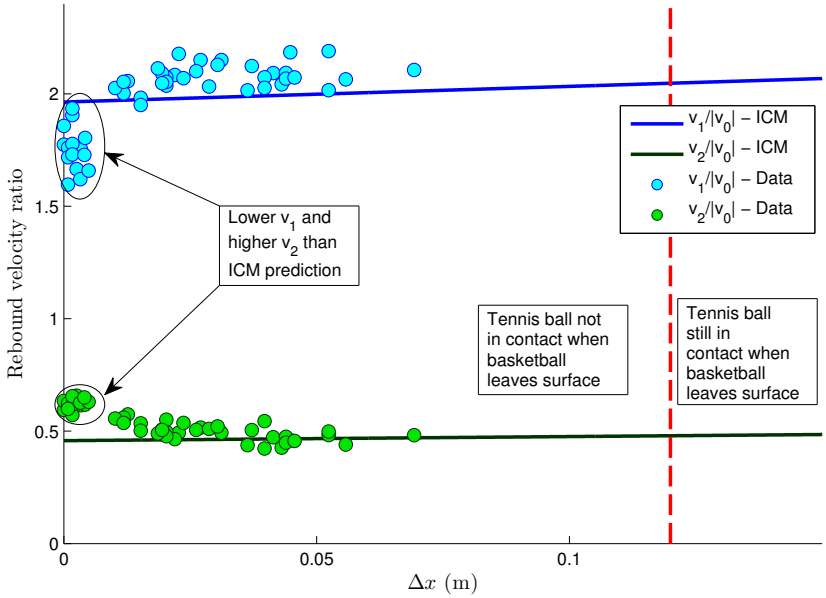

Figure 3. Basketball and tennis ball collision. Experimentally observed rebound velocities of the upper and lower balls, expressed as a proportion of the incident velocity v_0 of the basketball onto the floor. The near horizontal lines depict the ICM prediction. Note the breakdown of the ICM theory as $\Delta x < 10$ mm.

3. Continuum Elastic Model

The observed behaviour indicates that the ICM breaks down when the separation distance is very small and the mass ratio is much less than 1. We develop a model to describe the limiting case where $\Delta x \to 0$ and $\mu \to 0$. In order to do this we consider the lower ball to be a spherical elastic body.

There are several modelling choices to be made depending on which idealisation we make for the lower ball. The simplest case is to consider the body to be a spherical membrane, assuming that bending stiffness can be neglected. This approximation seems reasonable in case where the stiffness in the lower ball is mainly due to the internal pressure, for instance in the case of a basketball as in our experimental data. Evidence from measurements of force waveforms during high-speed impact with a force plate indicates that even hollow rubber balls with greater wall stiffness exhibit negligible bending during initial contact. [20].

An alternative choice would be to use classical shell theory (see [21,22]), including bending stiffness. The equation for free vibrations then becomes a sixth-order PDE. Considering the elastic response of the shell to initial conditions in space one obtains the same modes shapes as the analysis below using membrane theory, namely Legendre polynomials [23]. However, the dispersion relation becomes more complex. This theory could be applied in the case where bending stiffness dominates (for instance, if the lower ball is a rubber ball with approximately atmospheric internal pressure such as a pressureless tennis ball or table-tennis ball).

Another option would be to treat the lower body as a solid elastic ball. In this case the PDE for free vibrations now has an extra dependent variable which results in the Bessel functions appearing in the eigenfunctions (see [24]). For each eigenvalue there is now an infinite number of independent eigenfunctions and our dispersion relation becomes dependent on the spherical Bessel roots. One could apply this theory in the case where the lower ball is a superball, for instance.

The radial vibrations $u(t,\phi,\theta)$ of a spherical membrane can be described by the a wave equation of the form

$$\rho u_{tt} = T\Delta_s(u) + \text{damping} \tag{3.1}$$

where ϕ is polar and θ azimuthal, ρ is the surface density of the membrane and T is its tension (see e.g. [24]). Here the spherical Laplacian is defined as

$$\Delta_s(u) = \frac{1}{R^2}\left(\frac{\partial^2 u}{\partial\phi^2} + \cot(\phi)\frac{\partial u}{\partial\phi} + \operatorname{cosec}^2(\phi)\frac{\partial^2 u}{\partial\theta^2}\right)$$

where R is the sphere's radius. The damping in equation (3.1) will be defined later. Natural boundary conditions are that the radial displacement u must be bounded at the poles

$$u(t,0) = c_0, \quad u(t,\pi) = c_\pi \qquad \text{where} \qquad |c_0| < \infty, \quad |c_\pi| < \infty. \tag{3.2}$$

(a) Initial and lift-off conditions

The greatest challenge of the analysis is to define appropriate boundary conditions in time. Here we note from the stills of sports balls bouncing on rigid surfaces (see [14,25]) and our own experimental observations that there are two definite phases; a compression and a restitution phase. The compression phase involves the ball undergoing deformation as its region of contact with the ground expands and its kinetic energy is converted to elastic potential energy, resulting in the centre of mass velocity of the ball tending to zero. In contrast, the restitution phase involves the dissipation of the deformation energy into elastic waves which eventually cause the centre of mass velocity to reverse. Therefore we shall start our modelling when the compression phase is complete and the restitution phase is about to begin.

Specifically, we suppose that at time $t = 0$ the contact region of the lower ball is maximal and it has zero rigid body velocity (see Fig. 4), and that all the preceding kinetic energy of the falling ball has all been converted to elastic potential energy. We assume that the contact region with the ground is a circle, so that shape of the body is a sphere truncated at polar angle $\phi = \phi_a$. We also assume that the initial radial velocity (rate of dilation) is zero for all ϕ. Therefore we have

$$u(0,\phi,\theta) = RF(\phi) = RH(\phi-\phi_a)\left(\frac{\cos(\phi_a)}{\cos(\phi)} - 1\right) \quad \text{and} \quad u_t(0,\phi,\theta) = 0, \tag{3.3}$$

where H is the Heaviside step function and $\phi_a \in (\frac{\pi}{2}, \pi)$ remains to be determined. Note the axisymmetry of this initial condition means that we seek solutions to (3.1) that are independent of θ; $u = u(t,\phi)$.

A theoretical value for ϕ_a can be determined as a function of the rigid body velocity v_0 prior to impact through an energy argument, under the assumption that all rigid-body kinetic energy has been converted into deformation energy. Consider an infinitesimal piece of the membrane. Letting dp denote the pressure acting upon this piece we have

$$dp = dp(u) = T\Delta_s(u)du. \tag{3.4}$$

For simplicity, we assume a displacement process that increases linearly in time from 0 to u_0 in time τ, so that $u(t) = (t/\tau)u_0$. Then, the work done on this piece of membrane corresponding to displacement u_0 is

$$\delta W = \int_0^\tau p(t)\frac{du}{dt}dt = \int_0^{u_0} p(u)du.$$

Upon writing p as a function of time, we have $p(t) = p(u(t)) = T\Delta_s((t/\tau)u_0)$. Hence

$$\delta W = \int_0^\tau p(t)\frac{du}{dt}dt = \int_0^\tau T\Delta_s\left(\frac{u_0 t}{\tau}\right)\frac{u_0}{\tau}dt = \frac{T\Delta_s(u_0)u_0}{\tau^2}\int_0^\tau t dt = \frac{T}{2}u_0\Delta_s(u_0).$$

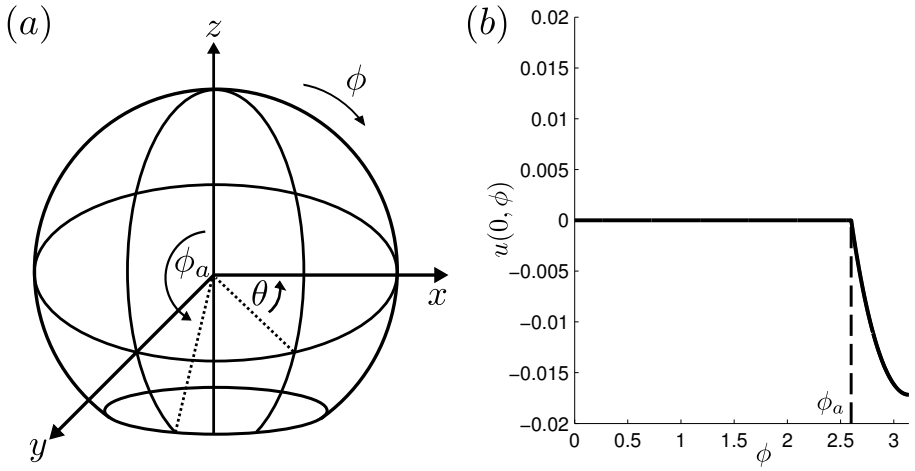

Figure 4. Assumed form of the initial condition in displacement. From (a) we can see that our initial condition does not depend on the azimuthal angle θ. (b) shows the radial displacement u at time $t = 0$ for $\phi_a = 2.6$.

The work done over the entire membrane can be calculated by replacing u_0 with the initial condition (3.3) and integrating over the sphere, yielding

$$W = -\int_S \delta W \, dS = -\int_S \frac{T}{2} RF(\phi)\Delta_s(RF(\phi)) \, dS$$
$$= -\frac{TR^2\pi}{3\cos(\phi_a)} \left(-1 + 2\cos^3(\phi_a) + 3\cos^2(\phi_a)\right). \tag{3.5}$$

From our earlier assumption we can equate the work done deforming the membrane with the kinetic energy prior to impact giving

$$\frac{1}{2} 4\pi\rho R^2 v_0^2 = -W. \tag{3.6}$$

Solving (3.5) and (3.6) for v_0, we have

$$v_0 = Rc\sqrt{\frac{-1 + 2\cos^3(\phi_a) + 3\cos^2(\phi_a)}{6\cos(\phi_a)}}, \tag{3.7}$$

$$\text{where} \quad c = \sqrt{T/\rho}/R \tag{3.8}$$

is the angular elastic wave-speed. This gives the desired relation between ϕ_a and v_0, which we shall test against empirical observation in §4 below.

To calculate the rebound velocity of the upper ball we need to find out at what time the impact process between the two ends and the balls separate. At $t = 0$ we assume that the upper body, a particle of infinitesimal mass, is resting at the top ($\phi = 0$) of the lower ball. The elastic wave in the lower ball propagates towards the top of the sphere until a time $t_l > 0$ at which the acceleration at $\phi = 0$ is sufficient for the particle to lift-off. We suppose that this happens for the smallest $t_l > 0$ such that the following two criteria are satisfied (see Fig. 5).

(i) **The contact force is zero.** Since we consider contact as a unilateral constraint, we predict the lift-off of one body from another when the contact force passes through zero and would become negative. We exclude the extremely rare case when the contact force is zero at a time instant but does not subsequently become negative. Specifically, in our mechanical model, as we have assumed the limit that upper body has infinitesimal mass,

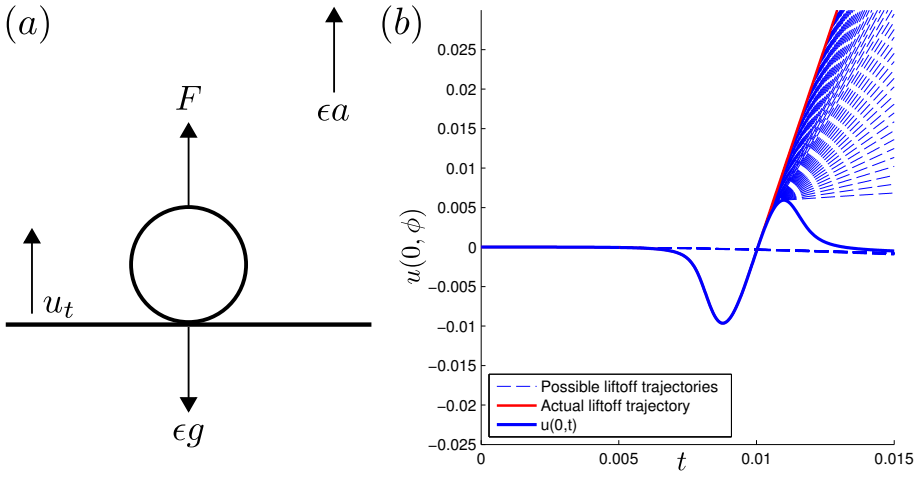

Figure 5. (a) Free-body diagram for a particle of small mass ϵ resting on a rigid surface that has a positive upwards velocity of u_t. (b) Illustrating a (non-physical) case where the upper point of the membrane is vibrating sufficiently violently for an 'early' tiny lift-off to be possible after applying the first two lift-off criteria. However the ensuing dynamics results in a second impact with the surface of the membrane. A range of possible lift-off points is indicated by the family of dashed curves. The chosen lift-off trajectory is the first one (indicated by a red solid line) that does not come back into contact with the membrane during the impact process we model.

the contact force will be zero when the membrane acceleration exactly cancels gravity. That is, $u_{tt}(t_l, 0) = -g$.

(ii) **There is no second impact.** While condition (i) is necessary and sufficient for lift-off, in practice multiple rapid impacts are possible. We have found such multiple impacts occur very rarely in the model provided there is sufficient damping and we have removed any spurious high-frequency oscillation (see 3.16 below). Also, our experiments did not detect any such behaviour. We therefore introduce a pragmatic condition, criterion (ii), that allows us to disregard such a situation. It is comprised of two sub-conditions. First, it is not reasonable to consider a negative lift-off velocity as we would instantaneously have a second impact. Second, assume the particle lifts off with a (small) $v_l = u_t(t_l, 0) > 0$. Then we need to check that there is not a subsequent time $\tilde{t}_l > t_l$ with $\tilde{t}_l - t_l = \delta t < t_l$ at which the particle comes back into contact with the membrane. The radial displacement of the particle for short times $t < t_l + \delta t$ after lift-off can be approximated as $s(t) = -\frac{1}{2}g(t - t_l)^2 + v_l(t - t_l) + u(t_l, 0)$. Thus we require $s(t) > u(t, 0)$ for $t_l < t < \tilde{t}_l$. From solely applying criterion (i) there could be a chattering sequence of multiple collisions and lift-offs. However, if we make the assumption that the upper body is approximately inelastic, it will only be the final lift-off velocity that is observed macroscopically (see Fig. 5). Criterion (ii) is applied to select this velocity.

(b) Solving the initial-value problem

In what follows, it is convenient to solve a dimensionless version of the problem by writing

$$u(t, \phi) = R\,\hat{u}(\hat{t}, \phi) \quad \text{and} \quad t = R\sqrt{\frac{\rho}{T}}\,\hat{t}.$$

We thus obtain the dimensionless wave equation

$$\hat{u}_{\hat{t}\hat{t}} - \hat{\Delta}_s(\hat{u}) + \text{damping} = 0, \qquad \text{where} \quad \hat{\Delta}_s = \left(\frac{\partial^2}{\partial\phi^2} + \cot(\phi)\frac{\partial}{\partial\phi}\right), \tag{3.9}$$

subject to initial conditions

$$\hat{u}(0,\phi) = F(\phi) = H(\phi - \phi_a)\left(\frac{\cos(\phi_a)}{\cos(\phi)} - 1\right), \qquad \hat{u}_t(0,\phi) = 0. \tag{3.10}$$

Lift-off occurs at the first time $\hat{t}_l$ such that

$$\hat{u}_{\hat{t}\hat{t}} = -\frac{Rg\rho}{T} := -\gamma,$$

which also satisfies the second two lift-off conditions. In what follows we shall exclusively deal with the dimensionless version of the equations, and will drop the hats. In order to compare with experiments in §4, however, all graphs and data will be given in terms of dimensional quantities.

The general solution of the axisymmetric spherical wave equation (3.9), in the absence of damping, can be obtained by the method of separation of variables, as in many textbooks (see e.g. [26,27]). Specifically we obtain

$$u(t,\phi) = a_0 + \sum_{n=1}^{\infty} a_n \cos(\omega_n t) P_n(\cos(\phi)) + b_0 t + \sum_{n=1}^{\infty} b_n \sin(\omega_n t) P_n(\cos(\phi)) \tag{3.11}$$

where $\omega_n = \sqrt{n(n+1)}$ and

$$P_n(x) = \frac{(-1)^n}{2^n n!}\frac{d^n}{dx^n}(1-x^2)^n$$

are the Legendre polynomials, which are subject to the orthogonality relations

$$\int_{-1}^{1} P_m(x)P_n(x)dx = \frac{2}{2n+1}\delta_{mn}.$$

The coefficients a_n and b_n are prescribed by the initial conditions (3.10). It is straightforward to see that zero initial velocity implies that $b_n = 0$ for all $n \geq 0$. Furthermore we have

$$a_n = \frac{2n+1}{2}\int_0^{\pi} F(\phi)P_n(\cos(\phi))\sin(\phi)d\phi, \tag{3.12}$$

and, in particular,

$$a_0 = \frac{1}{2}\int_0^{\pi} F(\phi)\sin(\phi)d\phi = \frac{1}{2}\left(\cos(\phi_a)\left(\log(-\cos(\phi_a)) - 1\right) - 1\right). \tag{3.13}$$

We next need to consider the effect of damping, which we shall introduce using a common engineering approximation, namely via introducing a mode-proportional viscous damping ratio (see e.g. [28–30]). That is, we assume there is a single viscous damping ratio D, such that each spatial mode $P_n(\cos(\phi))$ remains intact, but the time-dependent displacement in this mode obeys a second-order harmonic oscillator with undamped frequency ω_n that would be critically damped if $D = 1$. Using a damping ratio means that higher-frequency modes decay faster than modes of lower frequency. Specifically, assuming $0 < D < 1$, we find the solution to be

$$u(t,\phi) = a_0 + \sum_{n=1}^{\infty}\left(a_n\cos(\sqrt{n(n+1)}\sqrt{1-D^2}\,t) + b_n\sin(\sqrt{n(n+1)}\sqrt{1-D^2}\,t)\right) \mathrm{e}^{-D\sqrt{n(n+1)}\,t}P_n(\cos(\phi)) \tag{3.14}$$

where the a_n are identical to the un-damped case, given by (3.12) (3.13) and

$$b_n = \frac{(2n+1)D}{2\sqrt{1-D^2}}\int_0^{\pi} F(\phi)P_n(\cos(\phi))\sin(\phi)d\phi d\theta. \tag{3.15}$$

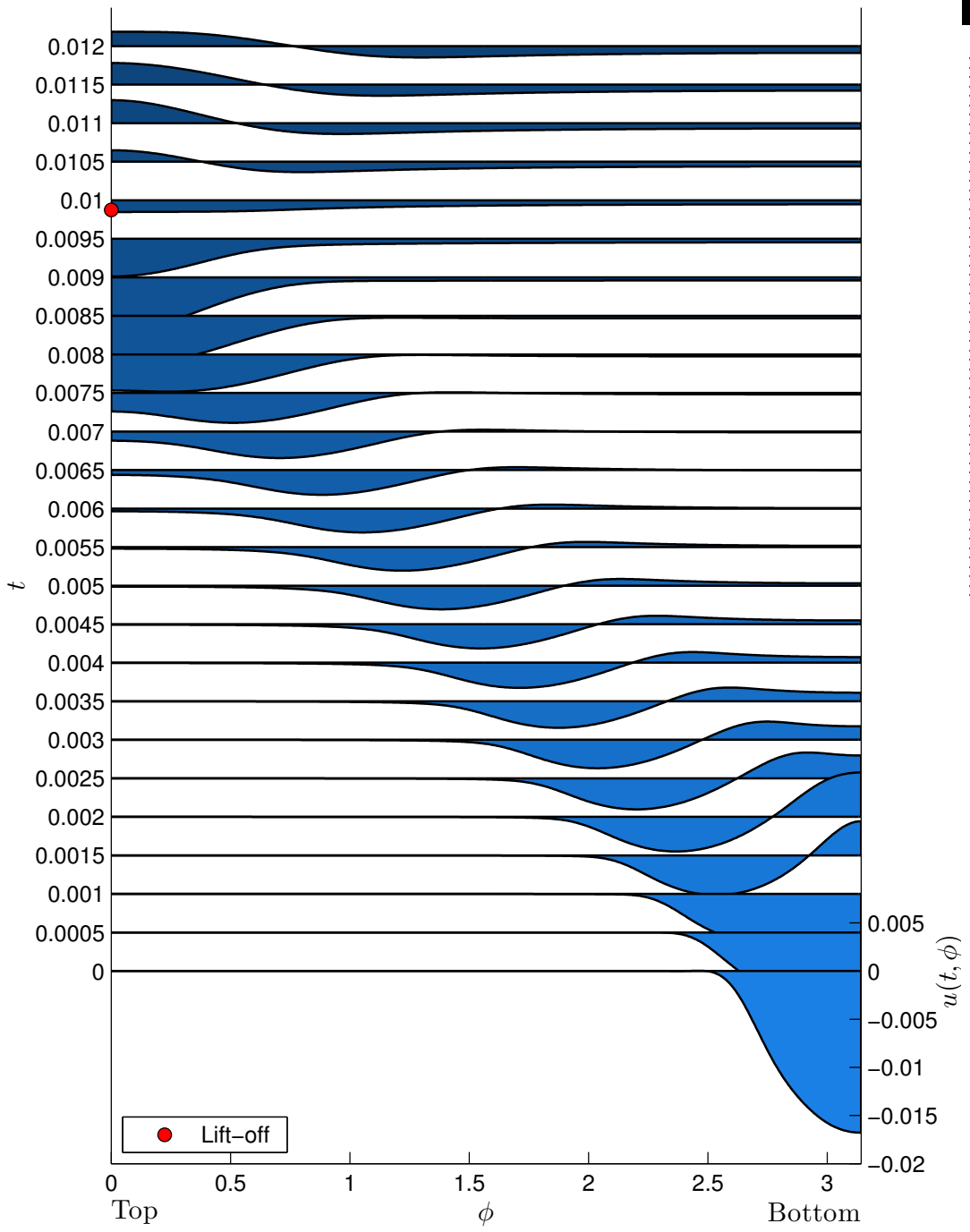

Figure 6. Representation of the radial displacement as a waterfall plot for 24 time instants. Parameters are $\phi_a = 2.6$, $R = 0.12$ m, $v_0 = -4.1$ ms^{-1}, $c = 320$ s^{-1}, $D = 0.1$.

Finally, in order to use (3.14) for practical prediction we need to truncate at some finite $n = N$. For the initial conditions (3.10), which are singular in derivative at $\phi = \phi_a$, we find that the sum converges slowly and there is also a significant Gibbs-like phenomenon. The Gibbs phenomenon is where the partial sums of a Fourier series of a piecewise continuously differentiable function

overshoot at a jump discontinuity. In particular, the overshoot approaches a finite limit as the frequency increases. It appears the phenomenon can be largely eliminated with the use of a Lanczos sigma factor, see e.g. [31]. Specifically the solution (3.14) is replaced by

$$u^{(N)}(t,\phi) = a_0 + \sum_{n=1}^{N} \sigma(n,N)\left(a_n \cos(\sqrt{n(n+1)}\sqrt{1-D^2}\,t) + b_n \sin(\sqrt{n(n+1)}\sqrt{1-D^2}\,t)\right) \mathrm{e}^{-D\sqrt{n(n+1)}\,t} P_n(\cos(\phi)), \quad (3.16)$$

$$\text{where} \quad \sigma(n,N) = \operatorname{sinc}\left(\frac{\sqrt{n(n+1)}}{\sqrt{N(N+1)}}\right) := \frac{\sqrt{N(N+1)}}{\sqrt{n(n+1)}} \sin\left(\frac{\sqrt{n(n+1)}}{\sqrt{N(N+1)}}\right)$$

and the coefficients a_n and b_n are given by (3.12), (3.13) and (3.15). With this approximation, we find that almost all the energy is contained in the first $N = 30$ modes which is the value of N used in all computations, unless otherwise stated.

Note that the solution (3.16) is expressed in closed form, and hence is readily evaluated using computer algebra. A typical solution is shown in Fig. 6. The final prediction for the lift-off velocity of the upper ball is thus given (in nondimensional terms) simply by the value of $u_t^{(N)}(t_l, 0)$.

4. Experimental comparison

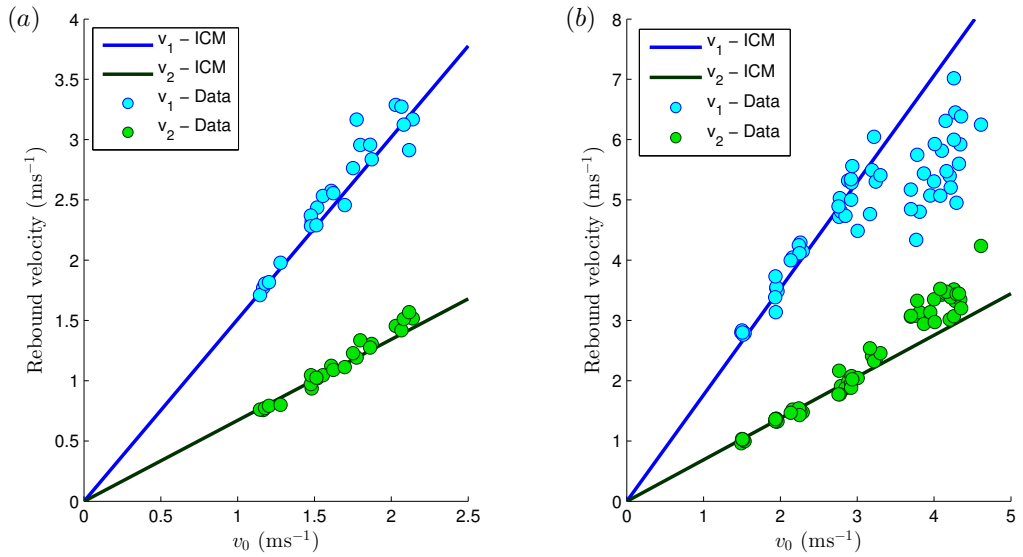

Figure 7. Tennis ball and light body impact in the case $\Delta x = 0$, for (a) a table tennis ball and (b) a coin. In each figure the solid lines give the prediction of the ICM (2.5).

In §2 we presented data on basketball/tennis ball impacts, which are unlikely to provide a good fit to the continuum theory because the mass ratio $\mu \approx 0.1$. We now present a more comprehensive set of experimental results using either a tennis ball or basketball as the lower ball, with various different light bodies forming the upper ball, in each case with a mass ratio much less than 0.1. See Table 1, the results in which we shall now explain in detail. The lighter bodies used included a UK one pence piece, a hexagonal steel nut of width approximately 5 mm and height 2 mm, a celluloid international standard 40 mm diameter table tennis ball and a scrunched up ball of tissue paper covered in cling film so that it retained an approximately spherical shape.

For each pair of colliding bodies, for a given initial separation Δx we found that the ratio of the post-impact to pre-impact velocity of either body was largely independent of the magnitude of the pre-impact velocity, provided this was not too high. See Fig. 7 for the case of the lower ball being a tennis ball. For each of the tennis-ball and lighter body cases, this ratio was also found to be largely independent of the initial separation distance Δx, providing it was not too large. Moreover, the recorded ratios were found to be broadly in line with the predictions of the ICM model (see the first three rows of Table 1).

For the basketball and lighter body cases though, a much stronger dependence on Δx was found, see Fig. 8. Typically, for Δx greater than about 25mm the observed rebound velocities were broadly in line with the ICM prediction (for both the upper and lower ball). However the velocity of the upper ball was greatly reduced for smaller Δx reaching a different, much lower, constant value for $\Delta x < 5$ mm. This value was roughly the same in the case that the upper ball was either the the tissue and table tennis ball, but was significantly greater for the tennis ball. As we shall see shortly, this lower lift-off velocity is consistent with the CEM prediction.

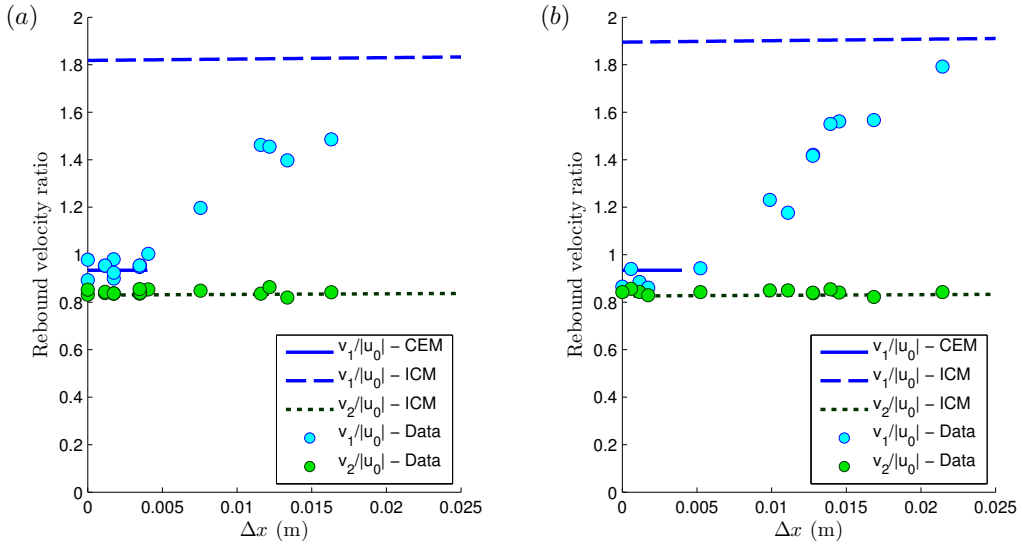

Figure 8. Basketball and light body impacts; illustrating the rebound velocity ratio for varying Δx for the (a) tissue ball (b) table tennis ball, respectively. The rebound velocity ratios are compared to those predicted by the ICM and the CEM. The height the balls fell through was kept constant at $x_2 = 0.92$ m. The smallest values of v_1, the rebound velocity of the upper body, occur in the limit $\Delta x \to 0$.

(a) Tennis ball and light body impacts; the success of the ICM model

In these experiments the two bodies were released so that they were just touching. This means that $\Delta x = 0$ so the prediction of the ICM is dependent solely on three parameters μ, e_2 and e_{12}. These were fitted independently and used to predict the rebound velocities of both balls, which could then be compared with the measured velocities. The mass ratio μ was obtained by weighing the two bodies. Then the coefficient of restitution of the tennis ball, e_2, was measured by repeatedly dropping it from different heights and comparing its velocity before and after impact. Similarly, the coefficient e_{12} was measured by repeatedly dropping the two bodies with sufficient separation distance so that they collided independently and then comparing relative velocities before and after collision. The mass ratios for each light rigid body and the measured coefficients of restitution with a tennis ball, e_{12} are given in the first three rows of Table 1.

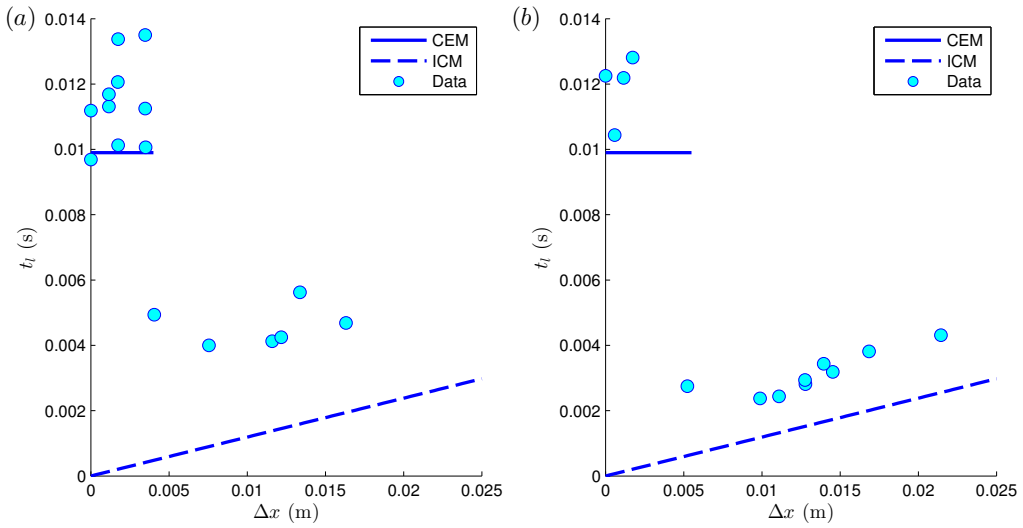

Figure 9. Basketball and light body impacts; Plotting the time to upper-body lift-off from maximum deformation of the basketball for (a) tissue and (b) table tennis ball. Note that for small Δx we have $t_l \in [0.009, 0.014]$ s. The value for t_l predicted by the ICM (see (2.2)) is the time between the impact of the lower ball and the floor and the impact between the two balls, as it makes the assumption each impact is instantaneous.

The two balls were then repeatedly dropped together, varying x_2 from 0.15 m up to 1 m, and the initial and final velocities were recorded. These velocities were subsequently compared with the prediction of the ICM (see Fig. 7), even though the separation distance is negligible so the assumptions of that theory do not strictly apply.

Positions were measured to the nearest pixel, which equates to en error of slightly less than ± 0.5 mm. All videos were recorded at 20,000 fps or greater and so, accounting for uncertainty over the choice of frame where the centre of mass velocity of the ball was zero, the accuracy of the measurement was to almost ± 0.1 ms. This results in errors of change in position measurements of ± 0.6 mm and errors of change in time measurements of ± 0.2 ms which means the velocity measurement is accurate to slightly less than 2 %. Therefore we obtain less than a 1 % error in measurements for the speed ratios. The masses of all balls were measured to ± 0.01 g. In Table 1) the speed ratios are given to two significant figures and the speed ratios are given to three significant figures. The coefficients of restitution were obtained from taking the linear best fit for a range of bounces and are given to two significant figures.

Table 1. Parameter values for the ICM with different balls. Also given is the recorded best fit to $v_1/|u_0|$ and $v_2/|u_0|$ in the case $\Delta_x \to 0$. This is compared with the prediction of the ICM model for the same quantity.

Lower	Upper	μ	e_2	e_{12}	$v_1/\|u_0\|$	ICM	$v_2/\|u_0\|$	ICM
Tennis	Coin	0.062	0.83	0.46	1.6	1.5	0.69	0.67
Tennis	Nut	0.035	0.83	0.41	1.5	1.5	0.74	0.74
Tennis	Table tennis	0.050	0.83	0.59	1.5	1.8	0.77	0.69
Basketball	Tennis	0.101	0.80	0.89	1.8	2.1	0.61	0.56
Basketball	Tissue	0.004	0.90	0.56	1.1	1.8	0.84	0.83
Basketball	Table tennis	0.005	0.90	0.60	1.2	1.9	0.84	0.83

In the two cases of the tennis ball with coin and tennis ball with nut (not shown) there is a good fit between the ICM and data (see Table 1 and Fig. 7(a)). At lower speeds there

appears to be a good fit for the tennis ball with table tennis ball as well. However at higher velocities there appears to be a clear discrepancy between the data and the ICM predictions (see Fig. 7(b)), possibly due to either nonlinear hardening or amplitude-dependent damping at larger amplitudes.

(b) Basketball and light body; parameter fitting the CEM model

Similar experiments were carried out for the basketball and light body, varying not only the drop height x_2, from 0.1 m to 1 m in intervals of 0.1 m, but also the initial separation from zero to 250 mm.

For each of the light bodies, as expected the basketball rebounds with almost the same velocity as it would when just dropped by itself. However, in the lower separation distance limit, as $\Delta x \to 0$, the velocities predicted by the ICM for the rebound of the lighter upper body are much higher than those measured (see Fig. 8), yet it appears that the measured rebound velocities of the upper body approach the ICM as the separation distance increases. Additionally, most of the impacts with low rebound velocity of the upper ball appear to have a much longer impact duration (see Fig. 9). The late lift-off in the limit as $\Delta x \to 0$ is not consistent with the ICM; in this limit the ICM would predict instantaneous lift-off. As the separation distance increases, the measured impact duration has better agreement with the ICM prediction.

Let us now attempt to assess the validity of the CEM model in explaining these results. In order to be used predictively, we need to find values for several key parameters:

(i) R, the radius of the lower ball;
(ii) c, the angular wave-speed of the lower ball – or equivalently the ball's surface density ρ and tension T;
(iii) v_0, the rigid body velocity of the lower ball just before impact;
(iv) ϕ_a, the polar angle corresponding to the deformation of the lower ball;
(v) D, the mode-proportional damping ratio.

The first two parameters of these parameters can be considered fixed properties of the lower ball. Clearly R is simple to find. The value of $c = \sqrt{T/\rho}/R$, can be obtained by first finding T and ρ. We can find T from the excess pressure P, relative to atmospheric. Consider a spherical membrane in equilibrium. If the radius R is increased by dR the extra work is $dW = TdA - PdV$ where dA is the change in surface area and dV is the change in volume [32]. We know $dA = d(4\pi R^2) = 8\pi R dR$ and $dV = d(4\pi R^3/3) = 4\pi R^2 dR$. This means the work done becomes $dW = (T8\pi R - P4\pi R^2)dR$. In equilibrium we know $dW = 0$, which results in a formula relating internal pressure and tension, which we can rearrange to express the surface tension as $T = PR/2$. Similarly, we can find ρ from the mass and surface density of the lower ball, $\rho = m/(4\pi R^2)$.

The third and fourth parameters in the above list, v_0 and ϕ_a, vary from experiment to experiment, and can be measured directly using the high-speed camera. In addition, we have a theoretical relation between v_0 and ϕ_a, given by (3.7). Measuring both values thus allows us to have an independent verification of our solution, in particular the calculated value of c and the form of the assumption of perfect conversion from pre-impact kinetic energy to deformation energy in arriving at the assumed initial condition.

The most difficult parameter to estimate is the coefficient of damping D, which depends heavily on the material properties of the ball. In practice, the best way we have found to fit D is to take one data point — that is, one experiment, with one kind of upper body, at one initial height (but with zero separation Δx) — and fit the lift-off velocity of the upper body v_1 to the measured output. This same value of D, which is deemed to be a material property of the lower ball, can then be used in all subsequent calculations.

Using the basketball as the lower ball, Table 2 gives the values of all the parameters that are measured and indicates which parameters then represent the experimental prediction of the model. With this data we can plot the equation relating ϕ_a and v_0 (3.7) against the computed

Table 2. Parameters for CEM in the case of the basketball. In the specific case of the basketball light-body experiment, where the initial height remained constant ($x_2 = 0.92$ m), measured parameter values were $m = 0.567$ kg, $P =$ 77200 Pa, $v_0 = -4.1$ ms^{-1} and $\phi_a = 2.6$ giving $v_1/|v_0| \approx 0.9$ and $t_l \approx 0.01$ s.

Symbol	Name	Value	Units	How obtained
R	Radius of basketball	0.12	m	Measured
c	Angular wave-speed	320	s^{-1}	Measuring P, R and m Verified from v_0 and ϕ_a
v_0	Rigid body velocity of lower ball	Varied	ms^{-1}	Measured per impact
ϕ_a	Angle of deformation of lower ball	Varied	Radians	Measured per impact
D	Damping parameter	0.13	None	Fitted from v_1 once
t_l	Impact duration	Varied	s	Predicted
v_1	Velocity of upper body after impact	Varied	ms^{-1}	Predicted

value of c. For the basketball, the measured value of $c = 320$ s^{-1} gives a good fit with data; see Fig. 10. We can further check whether this value of c is consistent with the measured impact duration in the basketball light-body impact. We assume the wave begins from the lowest point of the basketball (i.e. $\phi = \pi$) and travels along the surface of the membrane to the top (i.e. $\phi = 0$). Therefore if we measure the time taken from the maximum deformation of the lower ball to lift-off of the upper body (t_l) we can find the an approximation to c, the angular wave-speed, by dividing the angle traversed (ϕ) by the impact duration. Experimental results using the basketball and lighter body (such as the tissue ball and the table tennis ball) indicate that as $\Delta x \to 0$ we have $t_l \in [0.009, 0.014]$ s (see Fig. 9). This corresponds to an angular wave-speed $c \in [220, 350]$ s^{-1}. Using the relation between v_0 and ϕ_a (3.7) we can compare our upper and lower bounds for c to the data (see Fig. 10). The measured c is comfortably between the two bounds.

Now we can fit D by using the rebound velocity v_1 for a measured bounce. For the basketball light-body impacts the balls were dropped from a height of $x_2 = 0.92$ m, and had impact velocities of about 4.1 ms^{-1}. These impacts correspond to a maximum deformation angle ϕ_a of around 2.6. Using these parameter values in the CEM we find for a measured lift-off velocity of $v_1 \approx 3.7$ ms^{-1} we require a damping constant of $D = 0.13$ (see Fig. 11). As a further independent check, we find the predicted impact duration to be 0.0099 s which is in good agreement with the data; see Fig. 9.

In summary then, the CEM model seems to provide a consistent explanation of the results for the touching basketball and light body two-ball bounce problem. It predicts both the time of impact and the lift-off velocity of the upper-ball; in this case specifically that the ratio of this lift-off velocity to the pre-impact velocity is approximately 0.9 for $x_2 = 0.92$. Note that this lift-off velocity is much lower than the velocity predicted by the ICM model in this case.

5. Parameter dependence of the CEM

As well as being heavily dependent on the damping ratio D (see Fig. 11) the predictions of the CEM depend strongly upon the initial velocity v_0 and the measured properties of the lower ball – its angular wave-speed c and radius R. To test the dependence of the CEM on a given parameter all other values were taken as constants, specifically those measured for the basketball, aside from the polar angle corresponding to maximum deformation (ϕ_a) which was altered to to ensure that (3.7) was still satisfied.

From Fig. 12 it is clear that for each value of the damping ratio, D, there are optimum values for $v0$, c and R corresponding to the largest rebound velocity ratio. This maximal value itself is independent of the varied parameter, but dependent on the damping ratio - as the damping is increased the maximum rebound velocity ratio decreases (see Fig. 11) so one would expect smaller rebound velocity ratios in a more heavily damped ball. In the case that $D = 0.13$, as measured for the basketball, we have specifically that $v_0 \approx 8.7$ ms^{-1}, $c \approx 180$ s^{-1} and $R \approx 0.075$ m predict a maximal rebound velocity ratio of around 1.02.

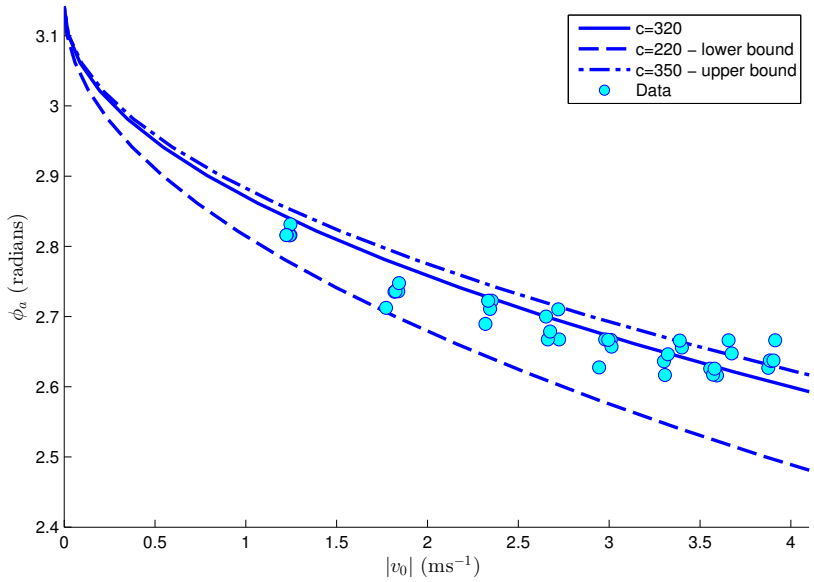

Figure 10. Deformation of basketball against initial velocity. We can use the equation relating ϕ_a and v_0 (3.7) to ascertain whether the value of the wave-speed obtained from measuring the pressure of the ball is reasonable for the CEM. Using this equation the measured value, $c = 320$ s^{-1}, gives a good fit to the data. We can also obtain approximate upper and lower bounds for the wave-speed by using the measured impact duration of the basketball light-body impact (see Fig 9 for the data). These bounds are plotted against the data. Our measured value for c lies within the two bounds.

As the initial velocity is proportional to the square root of the initial height x_0, in the case of the basketball it would appear that dropping it from a height of around $x_0 \approx 3.8$ m would result in the largest rebound velocity ratios. Interestingly, the value of wave-speed corresponding to the largest lift-off velocity ratio is actually lower than the measured value of c for the basketball. The angular wave-speed is proportional to the square root of the tension, T, which is directly proportional to the internal pressure, P, relative to atmospheric. The optimal value for the wave-speed is about $1/2$ of the value of c for the basketball, which corresponds to $1/4$ of the original pressure. Therefore the CEM predicts that deflating the basketball to slightly above atmospheric pressure would result in the maximal rebound velocity ratio. Also, according to the CEM, shrinking the radius of the basketball by around a third would result in the largest rebound velocity ratios.

From relation (3.7) we have that as a function of any given parameter ϕ_a follows an "S"-shaped curve, monotonically decreasing with v_0 but monotonically increasing with c and R. The former clearly makes sense physically - as v_0 increases the ball will deform more and so the polar angle of maximum deformation will decrease. Fig. 12 shows that as the damping is increased the values of c and R that correspond to the maximal rebound velocities decrease, and the value of v_0 increases. Consequently, increasing the damping and varying any single parameter (v_0, c or R) results in the value of ϕ_a associated with maximum rebound velocity ratios becoming smaller. This means that a more heavily damped ball requires greater deformation for the highest rebound velocity ratios.

It appears that decreasing the values of each parameter eventually results in a case where the upper body does not lift-off due to lift-off criterion (i) no longer being satisfied; the minimum acceleration of the point $\phi = 0$ on the lower ball never is lower than -9.81 ms^{-1}. In particular, for $D = 0.13$ as measured for the basketball, we have that there is no lift-off predicted for the three separate cases where $v_0 < 0.29$ ms^{-1}, $c < 13.3$ s^{-1} and $R < 0.091$ mm. As the damping ratio increases, these minimum values for lift-off for each parameter increase.

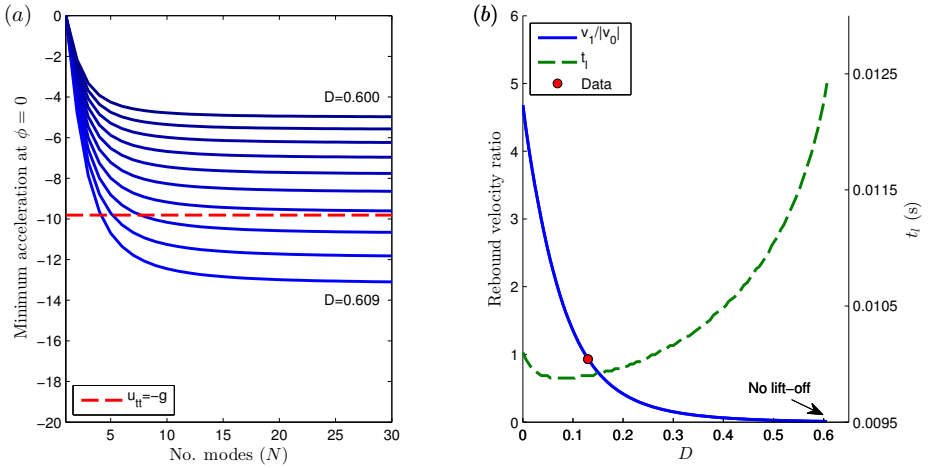

Figure 11. Computations using the CEM for $v_0 = -4.1$ ms^{-1}, $\phi_a = 2.6$, $R = 0.12$ m and $c = 320$ s^{-1}. (a) Minimum acceleration of the uppermost point of the lower ball for different values of the damping constant D (varying in 10 fixed increments from $D = 0.600$ to $D = 0.609$) and mode numbers N. If the minimum acceleration is never less than $-g$, the damping is too high for lift-off to occur. We can see that for $D > 0.602$, the CEM predicts that there is no lift-off. (b) CEM prediction of the rebound velocity and lift-off time t_l as the damping ratio D is changed for $N = 30$. The red dot indicates the fit to the basketball data - a value of $D = 0.13$ gives the required rebound velocity of around 3.7 ms^{-1}.

The lift-off time, t_l, predicted by the CEM is roughly independent of v_0 and R (data not shown). However we find that the faster the wave-speed of the lower ball, the smaller the predicted lift-off time. In particular it seems that $t_l \propto c^{-1}$.

6. Discussion

This paper has revisited a classical problem that has formed a popular classroom demonstration, which we have called *'the two-ball bounce problem'*, using careful experiments and a new elastic theory. Here the demonstrator drops two balls, a much lighter one on top of a heavy one from approximately chest height and invites the students to guess what happens next. Unless they have seen this before, no one tends to predict that the upper ball will hit the ceiling!

The first and perhaps most surprising conclusion is just how well the classical independent collision model (ICM), using measured coefficients of restitution, predicts the rebound velocities even in cases where its hypothetical impact sequence is not observed. In particular, for all separation distances $\Delta x < 120$ mm we observed a sequence of events such that: (i) the lower ball impacts with floor; (ii) the upper body impacts the lower ball; (iii) the upper body lifts off from the lower ball; (iv) the lower ball leaves floor. Yet for the basketball experiments in 4b) (see Figs. 9 and 8) the theory seems accurate down to $\Delta x \approx 25$ mm. In the case where the tennis ball was the lower ball, the ICM model prediction appears accurate all the way down to $\Delta x = 0$.

In the case of the lower ball being a basketball, there seems instead to be a different asymptotic limit which applies when $\Delta x < 5$ mm. This is characterised by lift-off times (that is the time from maximum deformation of the lower ball to lift-off of the upper ball) of about 0.01 s and rebound velocities that are significantly lower than those predicted by the ICM. To explain this we developed a new continuum elastic model (CEM). The various model choices we took include the use of membrane theory (rather than shell or solid elasticity theory) and an idealised form of initial condition. It would seem that these assumptions are justified in the case that the stiffness of the lower ball is dominated by internal pressure (as it is with a basketball, but less so with

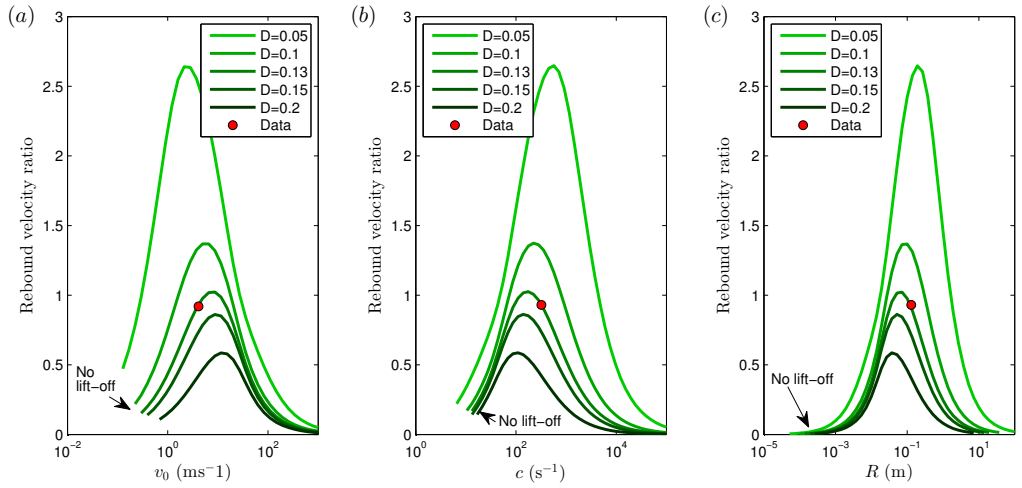

Figure 12. Computations illustrating the parameter dependence of the CEM. (a) $v_1/|v_0|$ for different values of the initial velocity, v_0, with parameters $R = 0.12$ m and $c = 320$ s^{-1}, choosing ϕ_a so that relation 3.7 is satisfied. (b) Similar to (a) but varying the angular wave-speed, c, with $R = 0.12$ m and $v_0 = 4.1$ ms^{-1} and ϕ_a chosen as before. (c) Again similar to (a), but varying the radius of the lower ball, R, with $v_0 = 4.1$ ms^{-1} and $c = 320$ ms^{-1}, choosing ϕ_a as in (a). In each subplot the red dot indicates the measured parameter value and corresponding rebound velocity for the basketball impact, and the green lines of different shades correspond to different values of the damping ratio, D.

a tennis ball). The fact that impact velocity and the angle ϕ_a could be measured independently in our experiments also provides an additional check that the initial conditions are reasonable. Nevertheless, it would be useful to test these assumptions more rigorously.

Estimating damping in continuum mechanics can be highly problematic, and we have found it easiest to make the (common) simplifying assumption of a mode proportional damping ratio. In reality, damping is likely to arise through material effects, but inclusion of such higher-derivative terms in the PDE (3.1) would have resulted in a far less tractable equation. Nevertheless, by comparison with one data point, we have been able to suggest a value for the damping constant D which gives approximately both the correct lift-off velocity and lift-off time. This is not quite as good as a truly independent validation of damping, but it was the best we could do given the experimental apparatus available.

For the cases of a basketball and a tissue ball and a basketball and a table tennis ball, the CEM model gave a good, consistent prediction. Note that this CEM prediction is independent of the properties of the upper body, provided that the mass ratio is sufficiently small (the theory does not take the mass of the upper ball into account). For the case of the basketball and tennis ball, while there is clearly an effect of a reduced lift-off velocity as $\Delta x \to 0$, the observed velocity is higher than the CEM prediction. This is perhaps not a surprise given that the mass ratio $\mu = 0.1$ in this case, which could hardly be described as small.

It would seem interesting to ponder why the tennis ball does not seem to show a different asymptotic behaviour as $\Delta x \to 0$. It is possible that it could all be a question of timing. The tennis ball was observed to have lower internal pressure than the basketball, and therefore the speed c of the travelling wave on its surface would likely be significantly slower than for the basketball. In this case, the "trampoline" effect does not occur soon enough before the rigid-body dynamics of impact takes over and the upper ball lifts off. To test this assumption carefully we would need to use spherical shell theory, which we also leave to future work. Alternatively, it could be that the mechanics of a tennis ball is too heavily damped. Using the basketball parameters with the CEM we found that if $D > 0.6066$ then there is insufficient energy in the travelling elastic wave to make

an upper body lift-off. All of this does not explain why the ICM model should be so accurate all the way down to $\Delta x = 0$ for the tennis ball, when the assumed event sequence of that model is violated for $\Delta x < 25$ mm. A proper explanation of this effect remains the subject of future work.

Returning to the basketball experiments, it is interesting that the CEM model prediction and indeed the experimental data show that there is a reduction in the lift-off velocity of the upper ball compared to the value obtained when the separation is larger. However, whereas the independent collision prediction for the velocity ratio between pre- and post-impact velocities is strictly bounded above by 3 (in the limit that both coefficients of restitution are unity), there is no such bound in theory for the CEM model prediction.

The CEM model could predict such large lift-off velocities for the upper ball in cases where the damping ratio is much smaller than that of the basketball. For a ball with identical properties to the basketball, the CEM model predicts a rebound velocity ratio of around 4.5 for the upper body (see Fig. 11) in the limit of no damping. Large velocity ratios could also be obtained from using a ball with the same damping ratio and radius as the basketball but with an angular wave-speed smaller by a factor of 1/2 (see Fig. 12).

We have not been able to produce very large lift-offs with the equipment we have used in the laboratory. But, presuming the CEM is correct, a membrane-like ball with lower internal pressure than a basketball (such as perhaps a volleyball or indoor football) might create a much larger effect, providing the damping is sufficiently small. It would also be good in future work to follow a similar procedure using a solid elastic model for the lower ball, which might apply to the case of a so-called superball.

In conclusion, it appears that even one of the simplest cases of multi-body chain collision impact, the 'two-ball bounce problem', still has plenty of mysteries left to be explored.

Acknowledgement

The authors would like to thank Chris Budd of the University of Bath for suggesting this problem of study, Clive Rendall for assistance with the experimental work, and participants at the John Ockendon retirement meeting for suggesting possible solution strategies after the problem was presented.

References

1. Stronge WJ. 2000. *Impact Mechanics*. Cambridge, UK: Cambridge University Press
2. Pfeiffer F, Glocker C. 1996. *Multibody Dynamics With Unilateral Constraints*. New York, USA: John Wiley & Sons
3. Chatterjee A, Ruina A. 1998. A New Algebraic Rigid-Body Collision Law Based on Impulse Space Considerations *J. Appl. Mech.* **65** 939–951 (DOI 10.1115/1.2791938)
4. Argatov, II. 2012. Mathematical modelling of linear viscoelastic impact: Application to drop impact testing of articular cartilage *Tribol. Int.* **63** 213–225 (DOI 10.1016/j.triboint.2012.09.015)
5. Seifried R, Schiehlen W, Eberhard P. 2010. The role of the coefficient of restitution on impact problems in multi-body dynamics *P. I. Mech. Eng. K* **224** 279–306 (DOI 10.1243/14644193JMBD239)
6. Huebner JS, Smith TL. 1992. Multi-ball collisions *Phys. Teach.* **30** 46–47 (DOI 10.1119/1.2343467)
7. Mellen W. 1995. Aligner for elastic collisions of dropped balls *Phys. Teach.* **33** 56–57
8. Harter WG. 1971. Velocity amplification in collision experiments involving superballs *Am. J. Phys.* **39** 656–663 (DOI 10.1119/1.1986253)
9. Müller P, Pöschel T. 2011. Two-ball problem revisited: Limitations of event-driven modeling *Phys. Rev. E* **83** 041304 (DOI 10.1103/PhysRevE.83.041304)
10. Cross R. 2007. Vertical bounce of two vertically aligned balls *Am. J. Phys.* **75** 1009–1016 (DOI 10.1119/1.2772286)
11. Patrício P. 2004. The Hertz contact in chain elastic collisions *Am. J. Phys.* **72** 1488–1491 (DOI 10.1119/1.1778394)
12. Hertz H. 1896. *Miscellaneous papers*. London, UK: Macmillan and Co

13. Falcona E, Laroche C, Fauve S, Coste C. 1998. Behavior of one inelastic ball bouncing repeatedly off the ground *Eur. Phys. J. B* **3** 45–57
14. Cross R. 1998. The bounce of a ball *Am. J. Phys.* **67** 222–227 (DOI 10.1119/1.19229)
15. Cross R. 2002. Grip-slip behaviour of a bouncing ball *Am. J. Phys.* **70** 1093–1102 (DOI 10.1119/1.1507792)
16. Bibó A, Károlyi G, Bódai T. 2009. Fly-wheel model exhibits the hither and thither motion of a bouncing ball *Int. J. Nonlinear Mech.* **44** 905–912 (DOI 10.1016/j.ijnonlinmec.2009.06.006)
17. Ismail KA, Stronge WJ. 2012. Viscoplastic analysis for direct impact of sports balls *Int. J. Nonlinear Mech.* **47** 16–21 (DOI 10.1016/j.ijnonlinmec.2012.02.007)
18. Hinch EJ, Saint-Jean S. 1999. The fragmentation of a line of balls by an impact *Proc. R. Soc. Lond. A* **455** 3201–3220 (DOI 10.1098/rspa.1999.0447)
19. Boechler N, Theocharis G, Job S, Kevrekidis PG, Porter M, Daraio C. 2010. Discrete Breathers in One-Dimensional Diatomic Granular Crystals *Phys. Rev. Lett.* **104** 244302 (DOI 10.1103/PhysRevLett.104.244302)
20. Cross R. 2014. Impact behavior of hollow balls *Am. J. Phys.* **82** 189–195 (DOI 10.1119/1.4839055)
21. Lamb H. 1882. On the Vibrations of a Spherical Shell *Proc. London Math. Soc.* **13** 50–56
22. Baker WE. 1961. Axisymmetric Modes of Vibration of Thin Spherical Shell *J. Acoust. Soc. Am.* **33** 1749–1758 (DOI 10.1121/1.1908562)
23. Kraus H. 1967. *Thin elastic shells*. New York, USA: John Wiley & Sons
24. Olver PJ. 2014. *Introduction to Partial Differential Equations*. New York, USA: Springer
25. Hubbard M, Stronge WJ. 2001. Bounce of hollow balls on flat surfaces *Sports Eng.* **4** 49–61 (DOI 10.1046/j.1460-2687.2001.00073.x)
26. Hassani S. 2013. *Mathematical Physics*. New York, USA: Springer
27. Zwillinger D. 1997. *Handbook of Differential Equations*. San Diego, USA: Academic Press
28. Fu Z, He, J. 2001. *Modal Analysis*. Oxford, UK: Butterworth-Heinemann
29. Ewins DJ. 2000. *Modal Testing: Theory, Practice and Application*. Exeter, UK: Wiley-Blackwell
30. Banks HT, Inman DJ. 1991. On Damping Mechanisms in Beams *J Appl. Mech.* **58** 716–723 (DOI 10.1115/1.2897253)
31. Hamming RW. 2000. *Digital Filters*. New Jersey, USA: Dover
32. Kane JW, Sternheim MM. 1991. *General Physics*. USA: John Wiley & Sons